Numerical simulation of the ocean general circulation and its climatic variability for the 1948-2007 using the INMOM

N.A. Diansky, A.V. Gusev

Institute of Numerical Mathematics
Russian Academy of Sciences
(INM RAS)

Outline

1. Short description of INMOM (Institute of Numerical Mathematics Ocean Model).
2. Results of experimetns in the scope of CORE program (Common Ocean Research Experiment - CORE-II): Global ocean simulation in 1948-2007.
3. Thermohaline circulation variability in North Atlantic and its relation with climate change.

The INMOM vertical coordinate is *σ* (like POM or ROMS), given by the expression:

$$\sigma = \frac{z - \zeta(x,y,t)}{H(x,y) - \zeta(x,y,t)}, \quad \sigma \in [0;1]$$

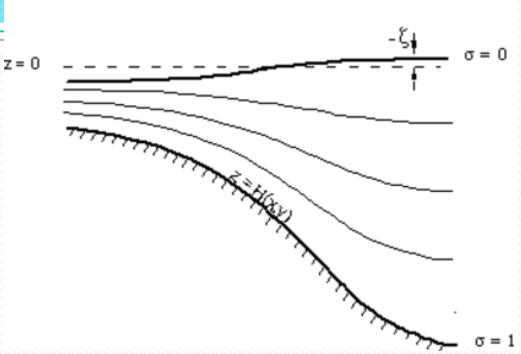

(x, y, z, t) -coordinates in *z*-system

(x_1, y_1, σ, t_1) -coordinates in *σ*-system

The equations are transformed from z- to σ- coordinate by implementing the transformation:

$$\frac{\partial}{\partial x} = \frac{\partial}{\partial x_1} - \frac{Z_x}{Z_\sigma}\frac{\partial}{\partial \sigma}, \quad \frac{\partial}{\partial y} = \frac{\partial}{\partial y_1} - \frac{Z_y}{Z_\sigma}\frac{\partial}{\partial \sigma},$$

$$\frac{\partial}{\partial z} = \frac{1}{Z_\sigma}\frac{\partial}{\partial \sigma}, \quad \frac{\partial}{\partial t} = \frac{\partial}{\partial t_1} - \frac{Z_t}{Z_\sigma}\frac{\partial}{\partial \sigma}.$$

$Z = \sigma h + \zeta$ - geopotential Z-depth as a function of model coordinates

$h = H - \zeta$ - effective ocean depth

ζ - sea level deviation from undisturbed state

The global version of the INMOM is realized on curvilinear orthogonal grid to avoid problems near North Pole.

Moebius transformation:

$$\eta = \frac{1 + A\xi}{\xi + A}$$

$$\xi = \tan\left(\frac{\pi}{4} + \frac{y}{2}\right)\exp(i(x - x_0)),$$

$$\eta = \tan\left(\frac{\pi}{4} + \frac{\varphi}{2}\right)\exp(i(\lambda - \lambda_0)),$$

$$A = \tan\left(\frac{\pi}{4} + \frac{\varphi_0}{2}\right).$$

$x_0, \lambda_0, \varphi_0$ -transformation parameters

New north pole is placed to 100°E, 70°N (Taimyr peninsula) and new south pole is symmetrically placed to 100°E, 70°S (Antarctica)

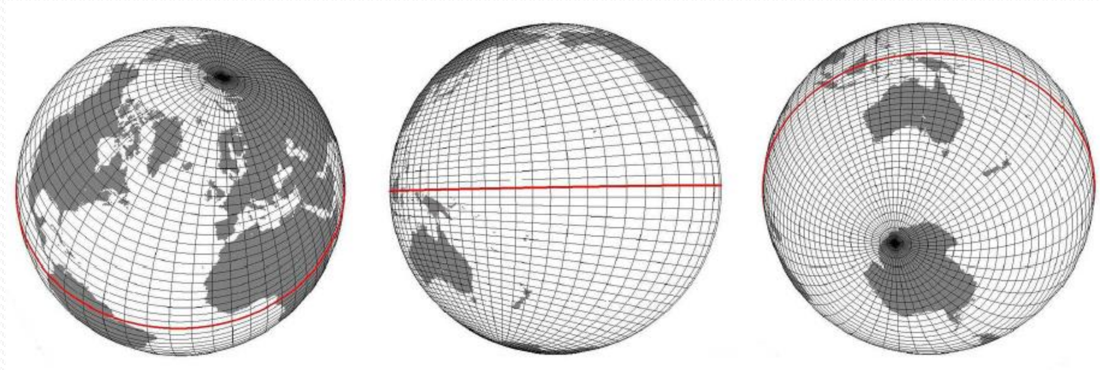

$$r_x = R\sqrt{\left(\frac{\partial\lambda}{\partial x}\cos\varphi\right)^2 + \left(\frac{\partial\varphi}{\partial x}\right)^2},$$

$$r_y = R\sqrt{\left(\frac{\partial\lambda}{\partial y}\cos\varphi\right)^2 + \left(\frac{\partial\varphi}{\partial y}\right)^2}.$$

- Metrical coefficients in curvilinear system

Global ocean bottom topography in the curvilinear coordinates

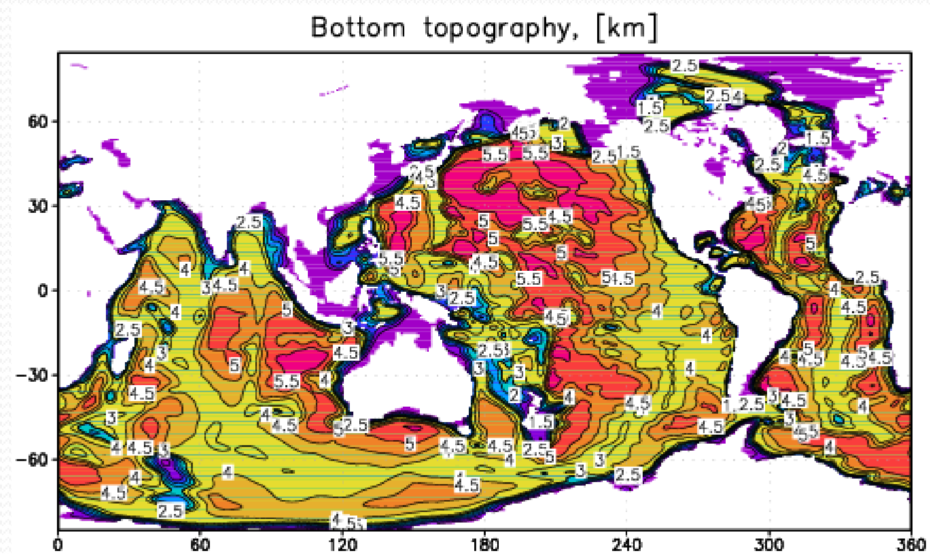

Grid properties:

1) Orthogonality (in horizontal coordinates)
2) Analytical transformation from geographical system
3) Singularities beyond the ocean area
4) Preserved geographical equator position

Parameters of Global version of INMOM are

1. Resolution is 1.0°x0.5° (360x340 nodes on horizontal grid and 40 σ-levels along depth) on the curvilinear grid with displaced poles (North pole is placed at 100°E 70°N).
2. Time step is 1 hour.
4. Initial conditions are rest state, January Levitus (1998) T and S, ice null.
7. Heat, salt and momentum fluxes at ocean surface were computed using CORE-II atmospheric data.
7. Sea ice dynamics-thermodynamics model (Yakovlev; Hunke, et. al) was used.
8. Lateral tracer mix is isopycnal diffusion 400 m^2/s
9. Lateral viscosity of 4-th order is approximately $2*10^5 m^4/s$
10. Vertical mix is Pacanovsky&Philander with simple wind wave breaking parameterization added.
11. SSS restoring of 50m/2yr is applied.

INMOM is used as oceanic component in INMCM4.0 for CMIP5 experiments for IPCC AR5

The experiment performed under CORE-II scenario

1. The run was started from Levitus climatology (1998).
2. Interannual CORE-II datasets for the period 1948-2007.
3. Five 60yr cycles were performed

North Atlantic Simulations in Coordinated Ocean-ice Reference Experiments phase II (CORE-II). Part I: Mean States

Gokhan Danabasoglu[a,*], Steve G. Yeager[a], David Bailey[a], Erik Behrens[b], Mats Bentsen[c], Daohua Bi[d], Arne Biastoch[b], Claus Böning[b], Alexandra Bozec[e], Vittorio M. Canuto[f], Christophe Cassou[g], Eric Chassignet[e], Andrew C. Coward[h], Sergey Danilov[i], Nikolay Diansky[j], Helge Drange[k], Riccardo Farneti[l], Elodie Fernandez[g], Pier Giuseppe Fogli[m], Gael Forget[n], Yosuke Fujii[o], Stephen M. Griffies[p], Anatoly Gusev[j], Patrick Heimbach[n], Armando Howard[f,q], Thomas Jung[i], Maxwell Kelley[f], William G. Large[a], Anthony Leboissetier[f], Jianhua Lu[e], Gurvan Madec[r], Simon J. Marsland[d], Simona Masina[m,s], Antonio Navarra[m,s], A. J. George Nurser[h], Anna Pirani[t], Davis Salas y Mélia[u], Bonita L. Samuels[p], Markus Scheinert[b], Dmitry Sidorenko[i], Anne-Marie Treguier[v], Hiroyuki Tsujino[o], Petteri Uotila[d], Sophie Valcke[g], Aurore Voldoire[u], Qiang Wang[i]

[a]*National Center for Atmospheric Research (NCAR), Boulder, CO, USA*
[b]*Helmholtz Center for Ocean Research, GEOMAR, Kiel, Germany*
[c]*Uni Climate, Uni Research Ltd., Bergen, Norway*
[d]*Centre for Australian Weather and Climate Research, a partnership between CSIRO and the Bureau of Meteorology, Commonwealth Scientific and Industrial Research Organisation (CSIRO), Melbourne, Australia*
[e]*Center for Ocean-Atmospheric Prediction Studies (COAPS), Florida State University, Tallahassee, FL, USA*
[f]*NASA Goddard Institute for Space Studies (GISS), New York, NY, USA*
[g]*Centre Européen de Recherche et de Formation Avancée en Calcul Scientifique (CERFACS), Toulouse, France*
[h]*National Oceanography Centre Southampton (NOCS), Southampton, UK*
[i]*Alfred Wegener Institute for Polar and Marine Research (AWI), Bremerhaven, Germany*
[j]*Institute of Numerical Mathematics, Russian Academy of Sciences, Moscow, Russia*
[k]*University of Bergen, Bergen, Norway*
[l]*International Centre for Theoretical Physics (ICTP), Trieste, Italy*
[m]*Centro Euro-Mediterraneo sui Cambiamenti Climatici (CMCC), Bologna, Italy*
[n]*Massachusetts Institute of Technology, Cambridge, MA, USA*
[o]*Meteorological Research Institute (MRI), Japan Meteorological Agency, Tsukuba, Japan*
[p]*NOAA Geophysical Fluid Dynamics Laboratory (GFDL), Princeton, NJ, USA*
[q]*Medgar Evers College of the City University of New York, Brooklyn, NY, USA*
[r]*IPSL/LOCEAN, CNRS-IRD-UPMC, Paris, France*

[*]Corresponding author. Tel.: +1 303 497 1604; fax: +1 303 497 1700.
Email address: gokhan@ucar.edu (Gokhan Danabasoglu)

Preprint submitted to Ocean Modelling *March 27, 2013*

Abstract

Simulation characteristics from eighteen global ocean – sea-ice coupled models are presented with a focus on the mean Atlantic meridional overturning circulation (AMOC) and other related fields in the North Atlantic. These experiments use inter-annually varying atmospheric forcing data sets for the 60-year period from 1948 to 2007 and are performed as contributions to the second phase of the Coordinated Ocean-ice Reference Experiments (CORE-II). The protocol for conducting such CORE-II experiments is summarized. Despite using the same atmospheric forcing, the solutions show significant differences. As most models also differ from available observations, biases in upper-ocean potential temperature and salinity distributions, mixed layer depths, and sea-ice cover in the Labrador Sea region are identified as contributors to differences in AMOC. These differences in the solutions do not suggest an obvious grouping of the models based on their ocean model lineage, their vertical coordinate representations, or surface salinity restoring strengths. Thus, the solution differences among the models are attributed primarily to use of different subgrid scale parameterizations and parameter choices as well as to differences in horizontal and vertical grid resolutions in the ocean models. Use of a wide variety of sea-ice models with diverse snow and sea-ice albedo treatments also contributes to these differences. Based on the diagnostics considered, the majority of the models appear suitable for use in studies involving the North Atlantic, but some models require dedicated development effort.

Keywords:
Global ocean – sea-ice modelling, Ocean model comparisons, Atmospheric forcing, Experimental design, Atlantic meridional overturning circulation, North Atlantic simulations

Climatic circulation characteristics (average for 1948-2007)

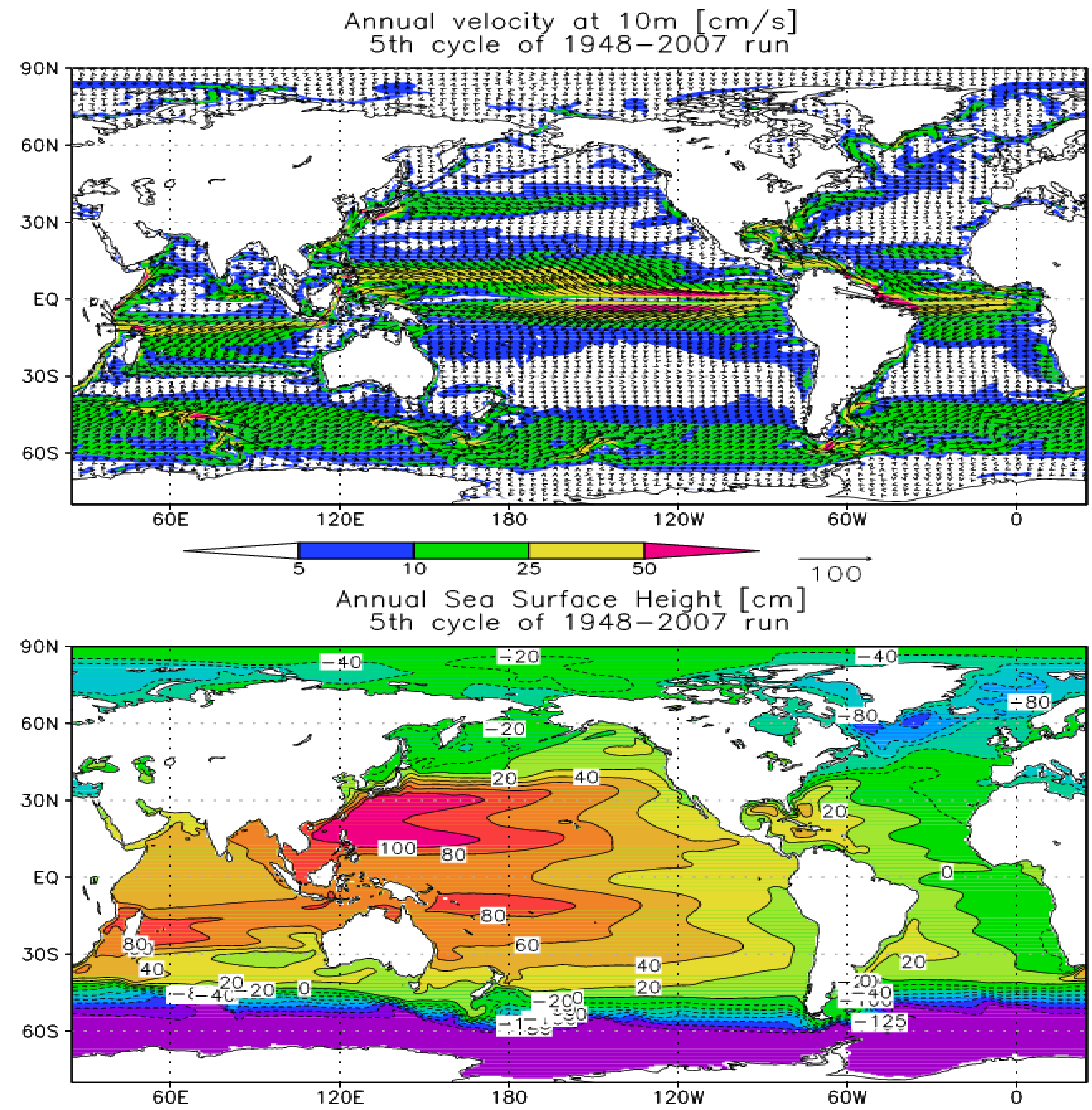

Equatorial circulation

INMOM (average for 1948-2007)

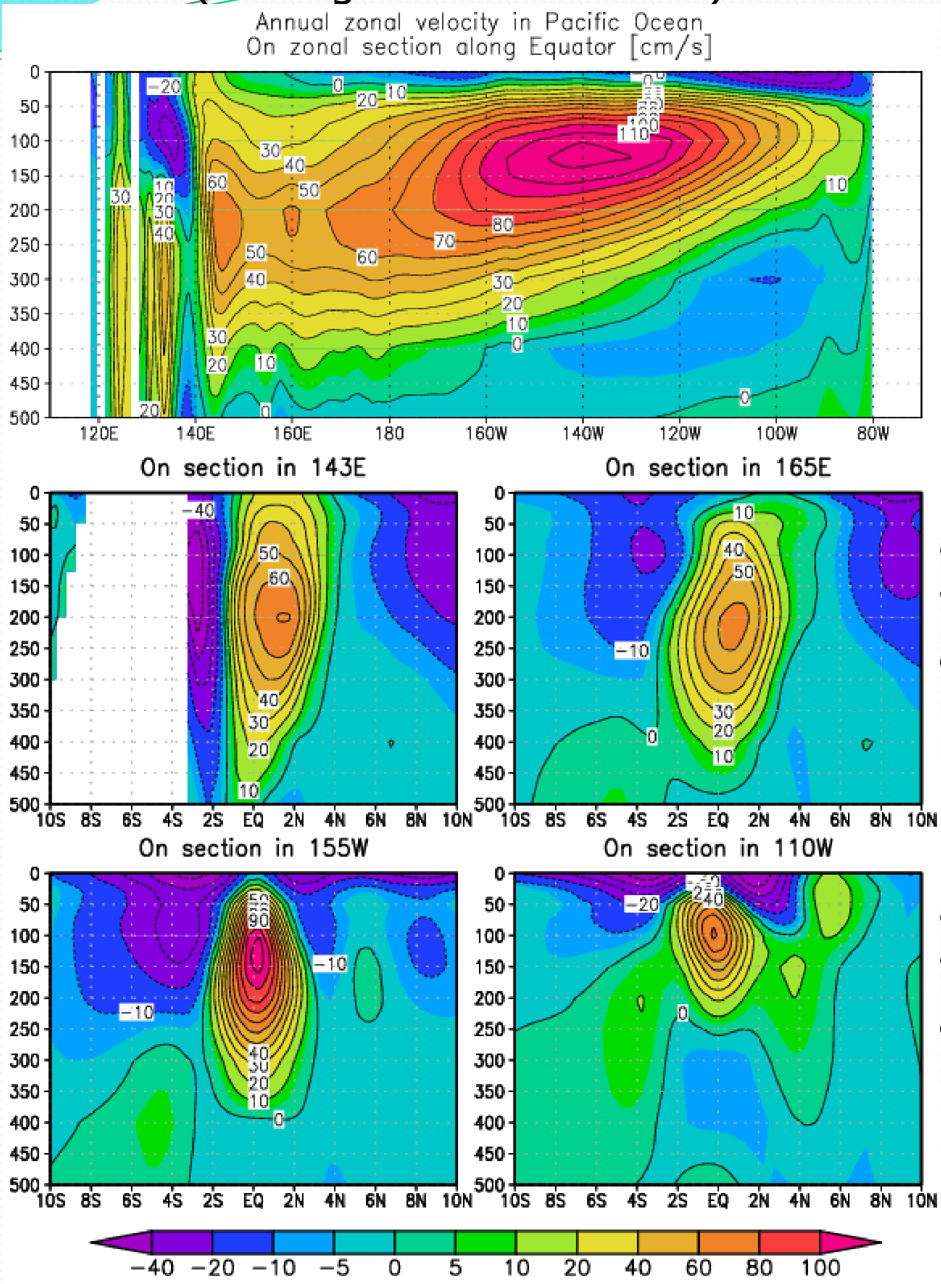

OFES(Masumoto et._al., 2004)
-high-resolution MOM

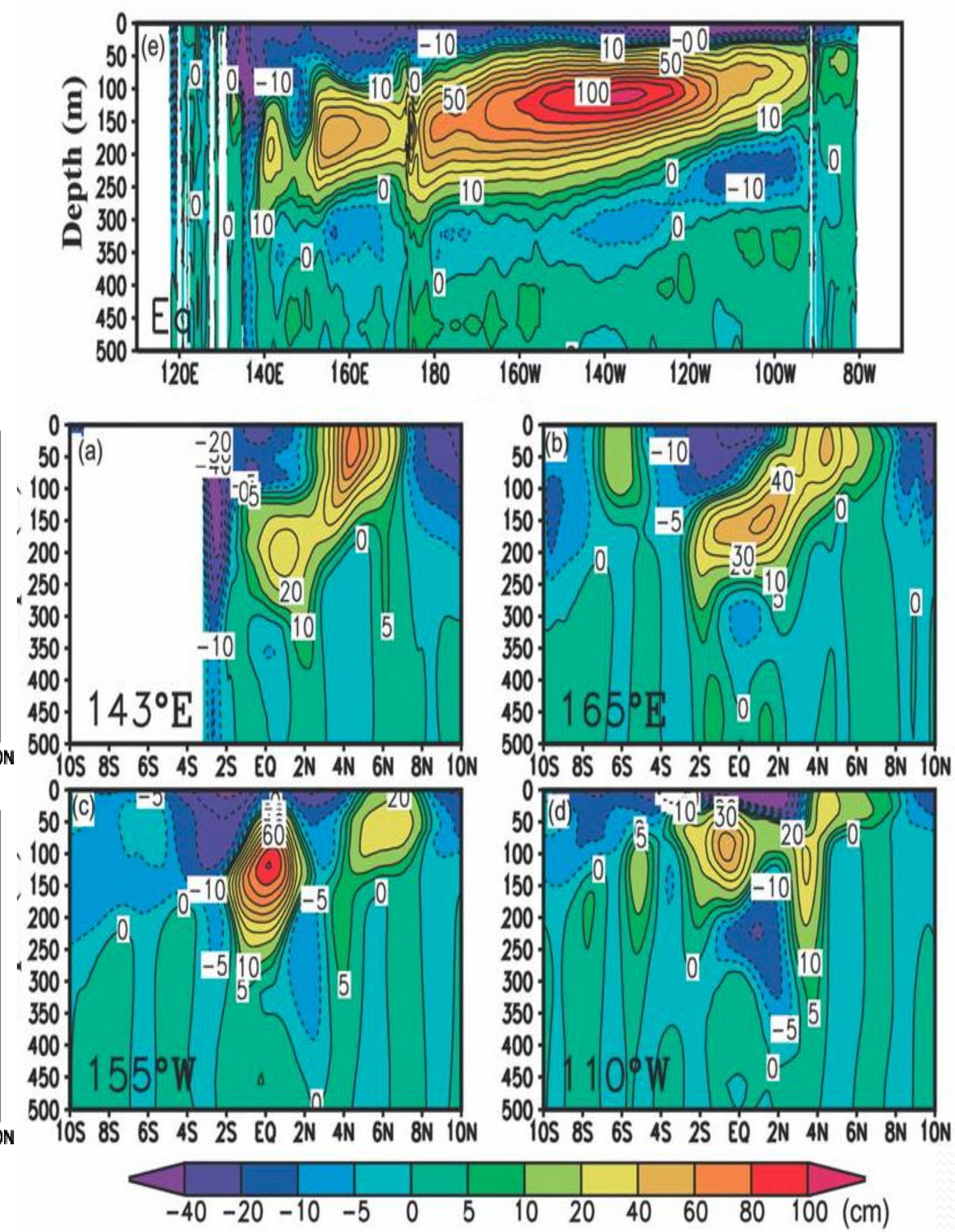

Sea ice in March

Площадь льда в марте, млн. кв. км

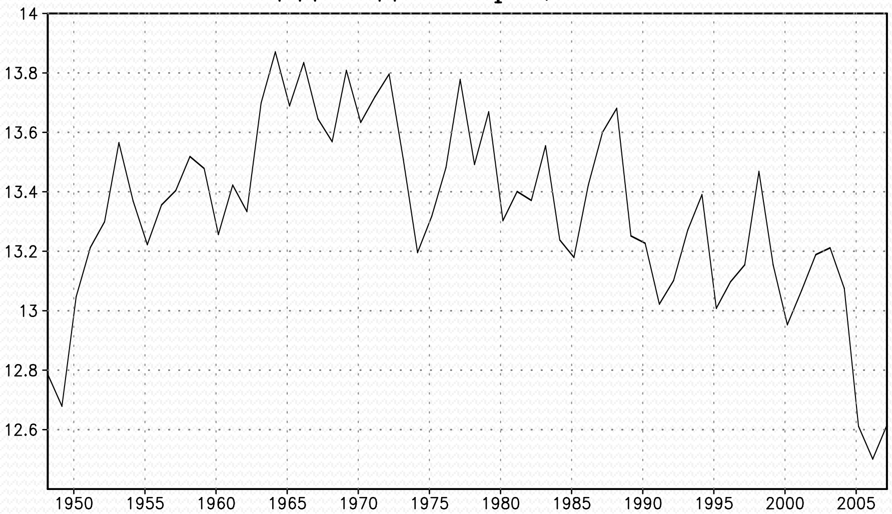

Объем льда в марте, трлн. куб. м

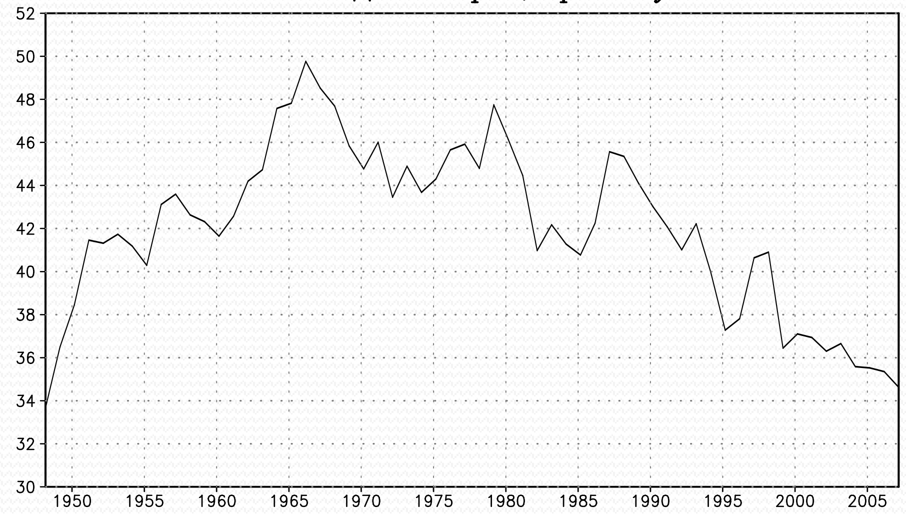

Среднемартовская концентрация льда за 1948–2007

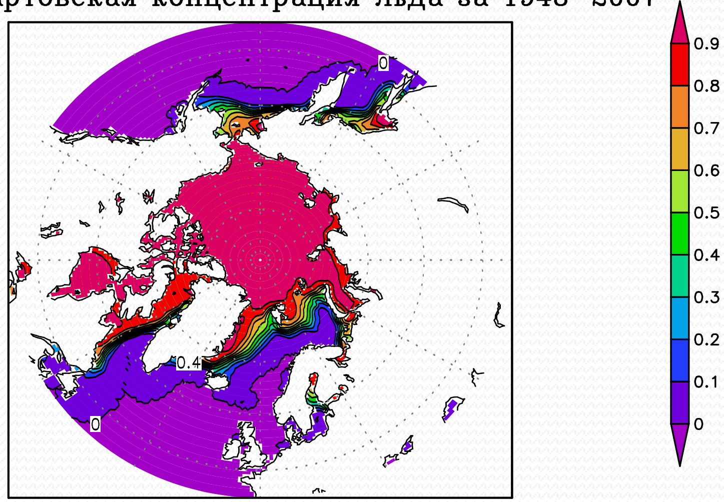

Среднемартовская толщина льда за 1948–2007, см

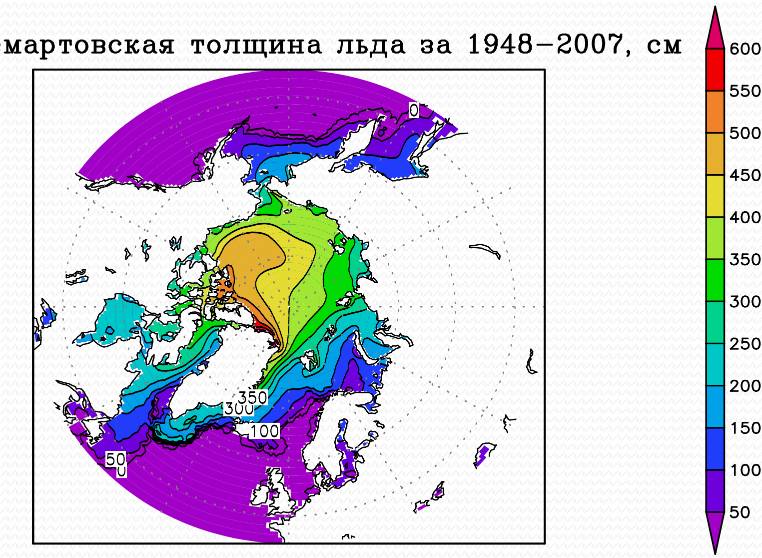

Sea ice in September

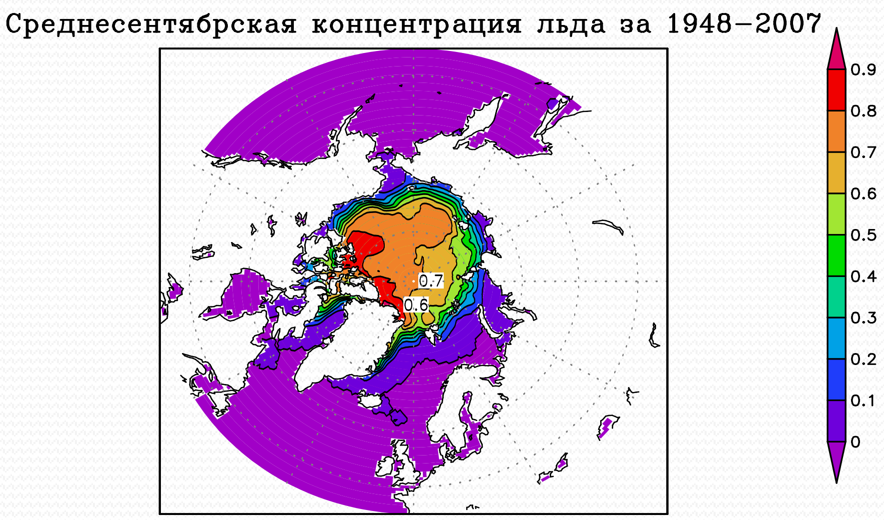

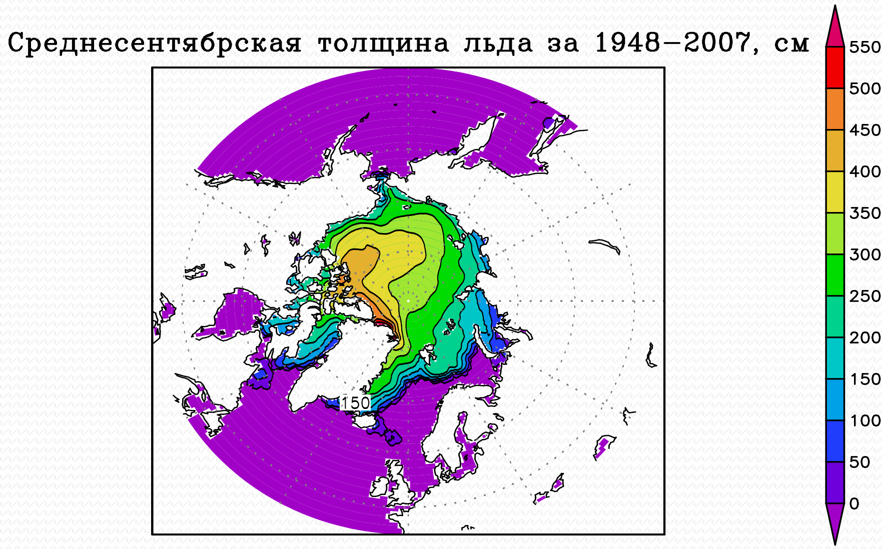

MOC streamfunction

INMOM (average for 1948-2007)

Annual mean global meridional overturning ciculation, Sv

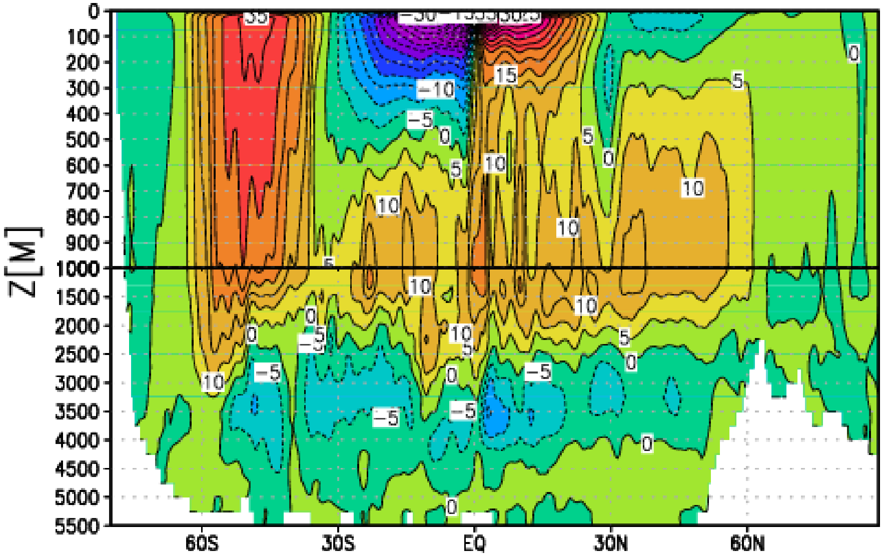

Annual mean Atlantic meridional overturning ciculation, Sv

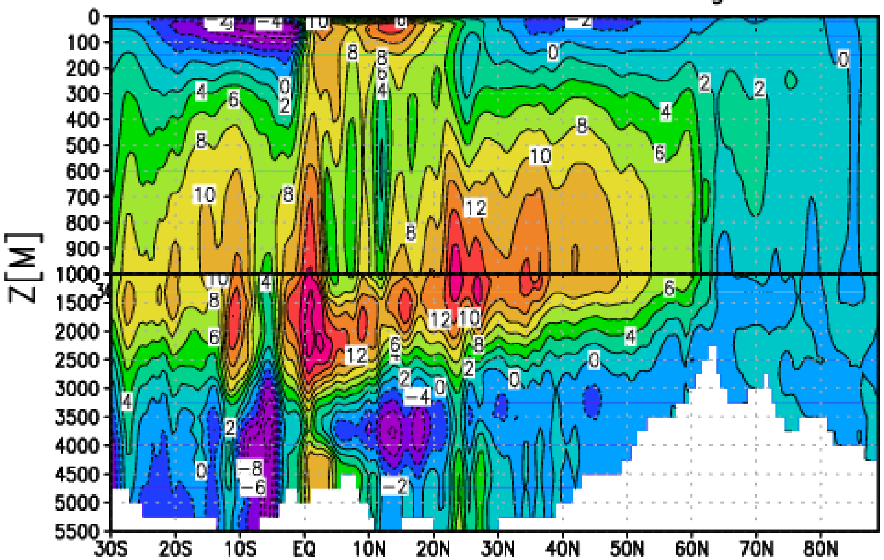

OFES(Masumoto et._al., 2004)
-high-resolution MOM

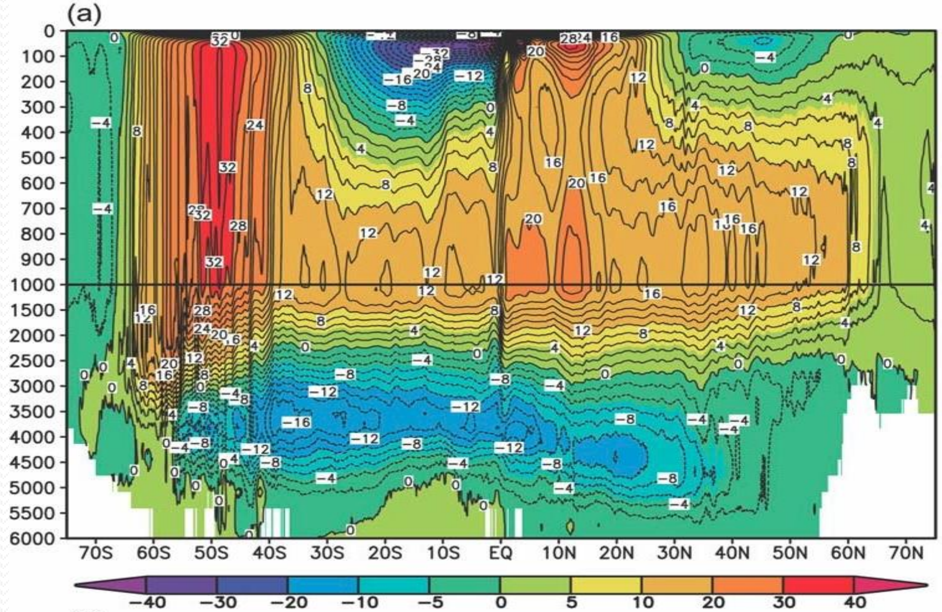

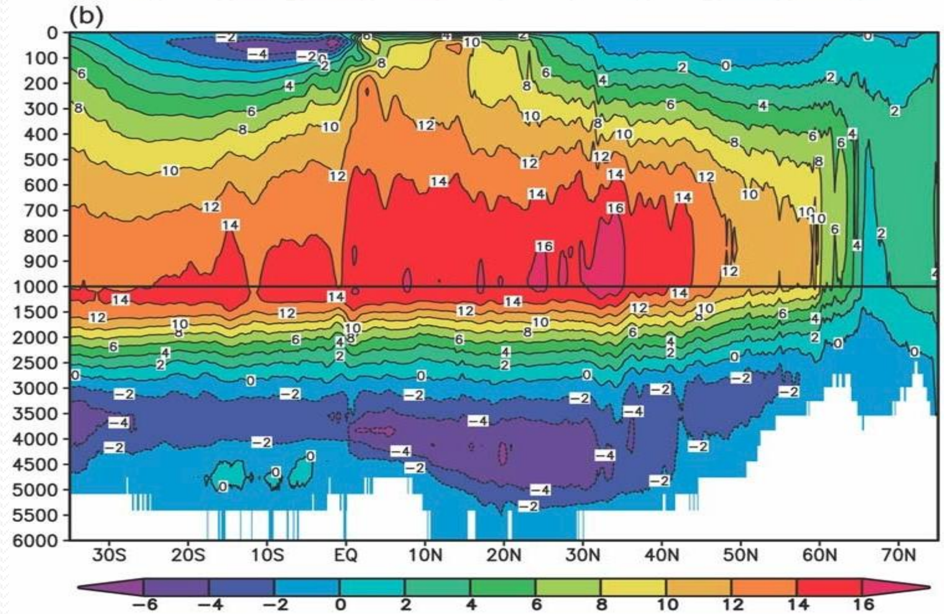

MHT

INMOM (average for 1948-2007)

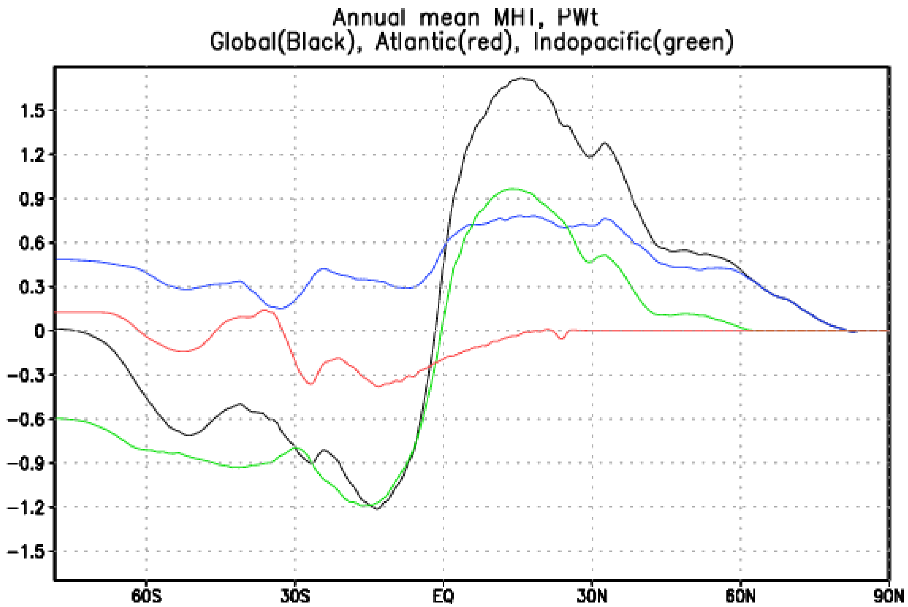

Estimations (Trenberth and Carron, 2001)

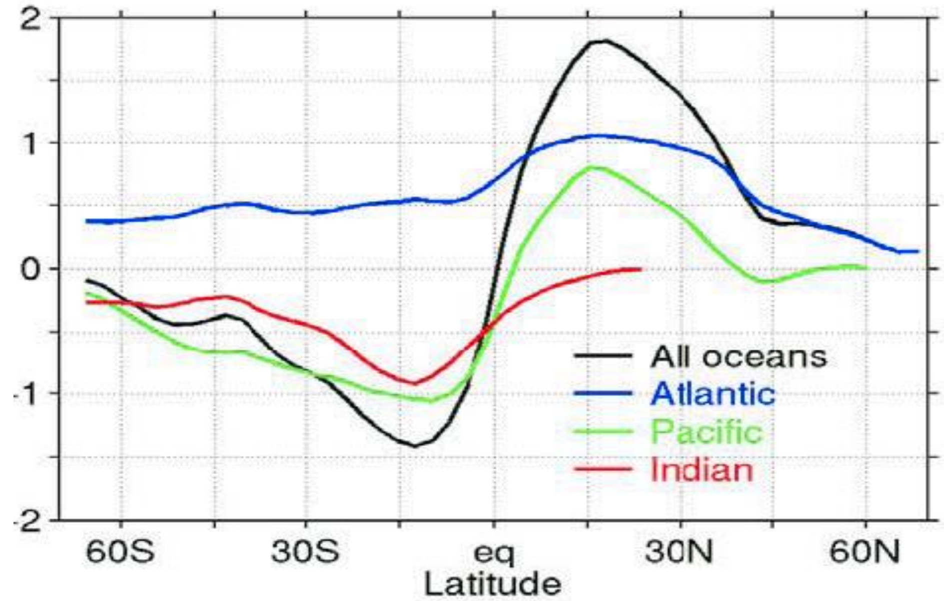

Atlantic Meridional Overturning Circulation

Figure 3: Time-mean AMOC plotted in depth (km) and latitude space. The positive and negative contours indicate clockwise and counter-clockwise circulations, respectively. Unless otherwise noted, the time-mean refers to the 20-year means for years 1988-2007, corresponding to simulation years 281-300, in all the figures.

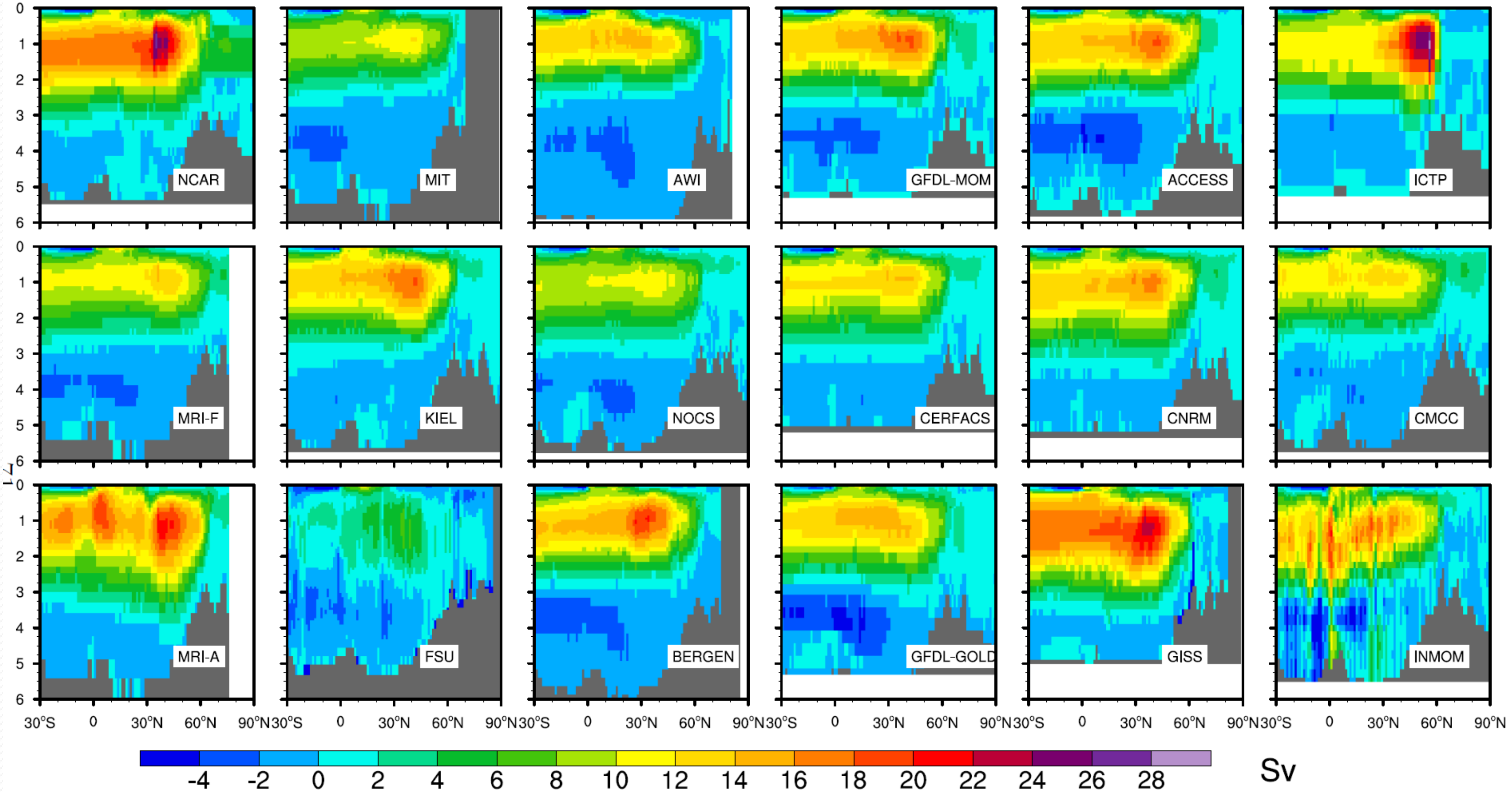

Индекс АМО за 1948-2007
Сплошная – модель, пунктир – наблюдения

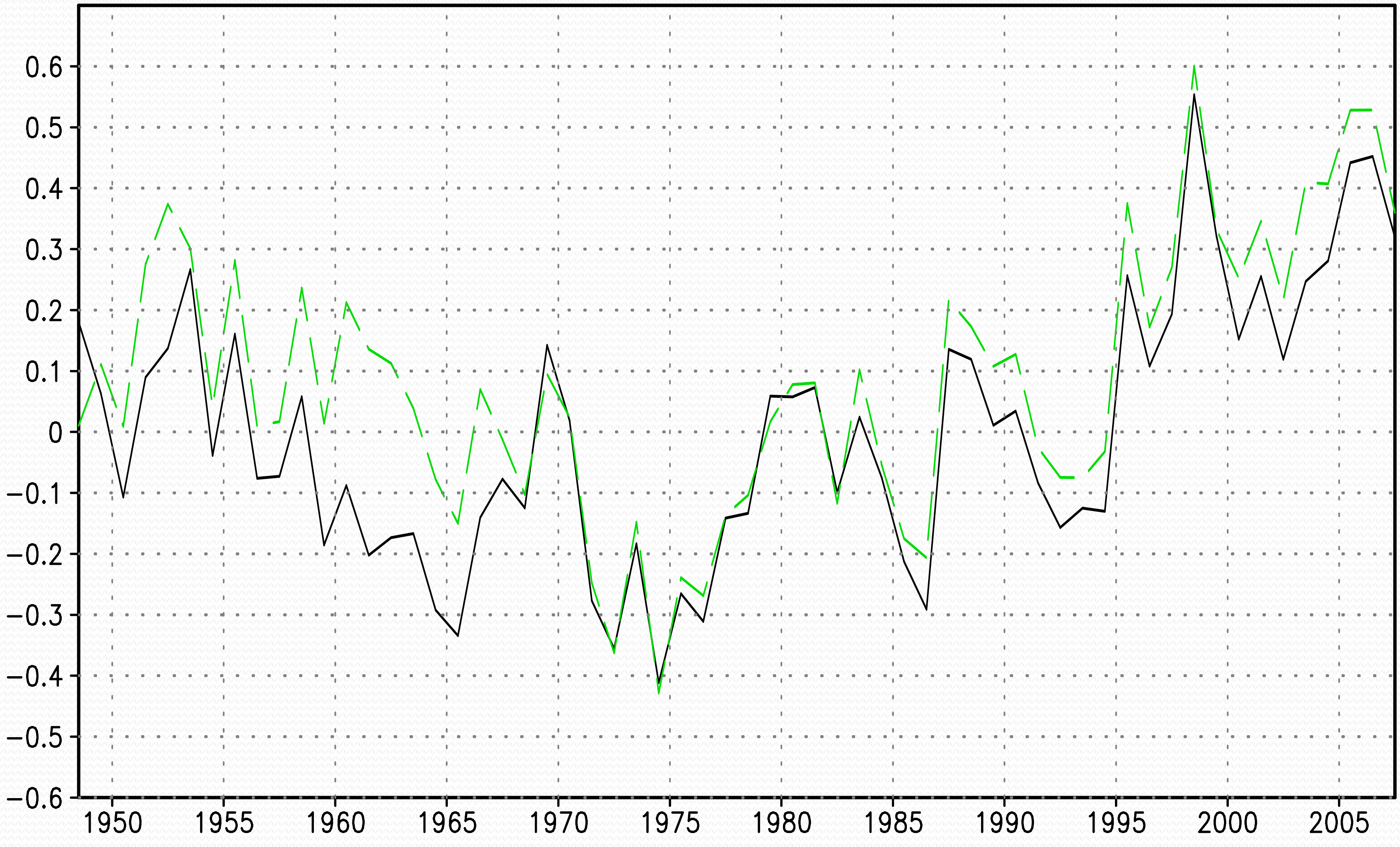

Индекс АТХЦ в Атлантике, Св

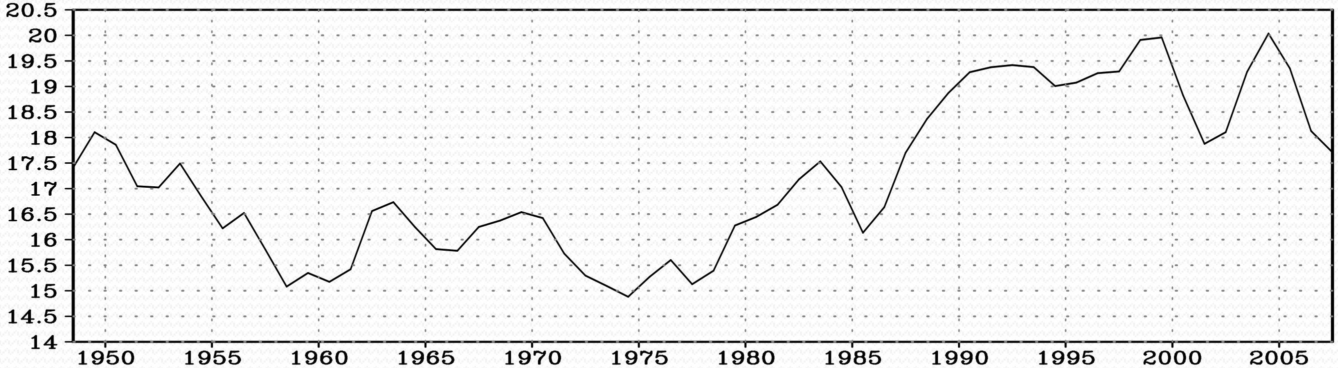

МПТ средний в 30–60с.ш. Атлантики, ПВт

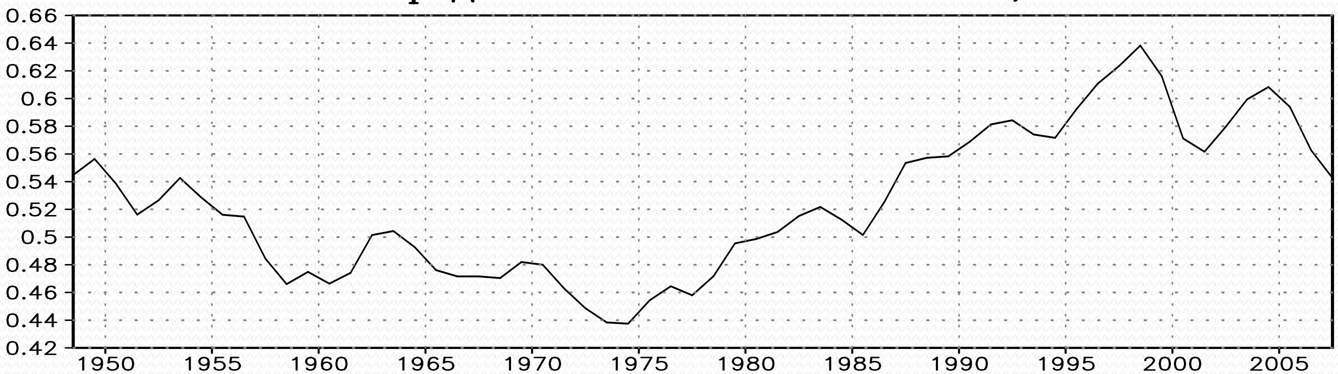

Полный поток тепла в атмосферу, Вт/кв.м

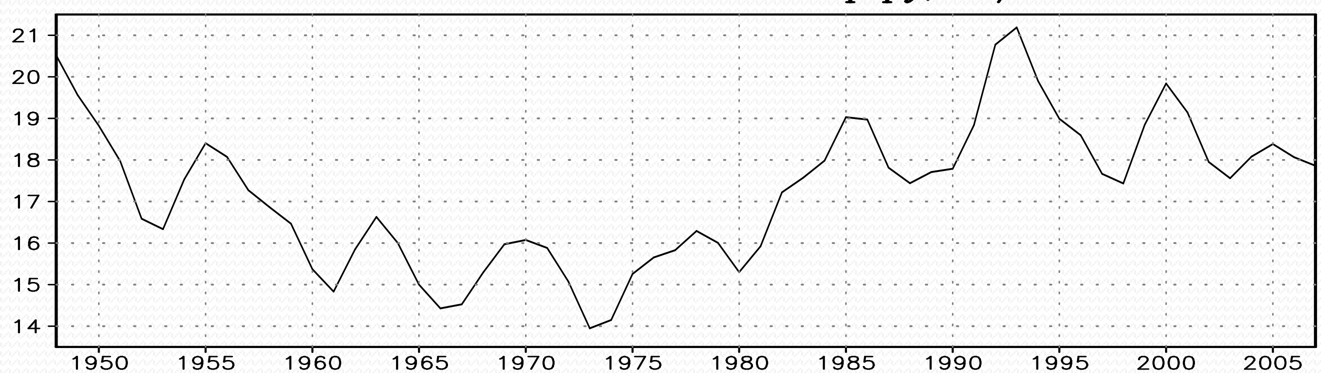

Global and Hemispheric Annual Temperature Anomalies
1850–2012

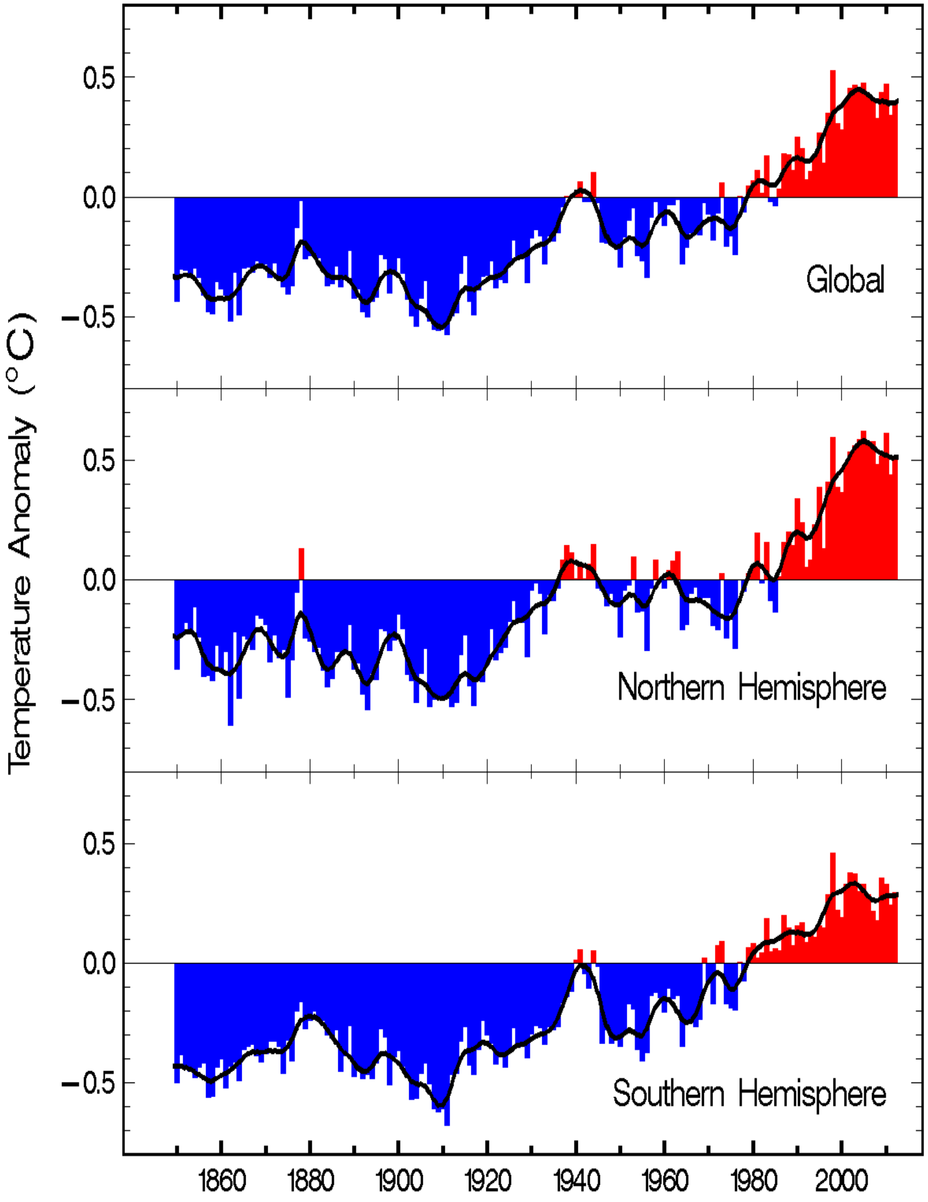

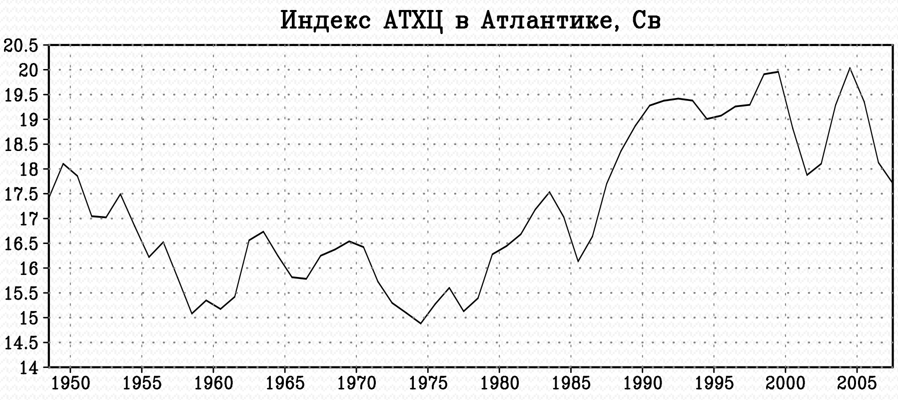

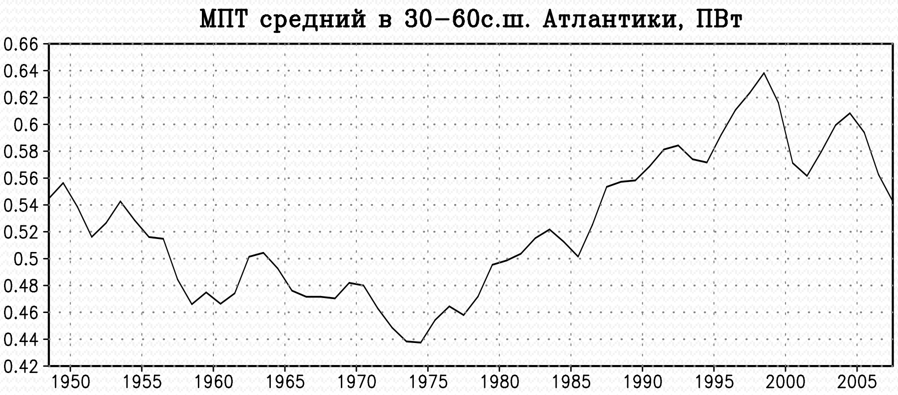

Power Spectra of max of annual North Atlantic MOC from 750-yr control run of INMCM4.0 (CMIP5)

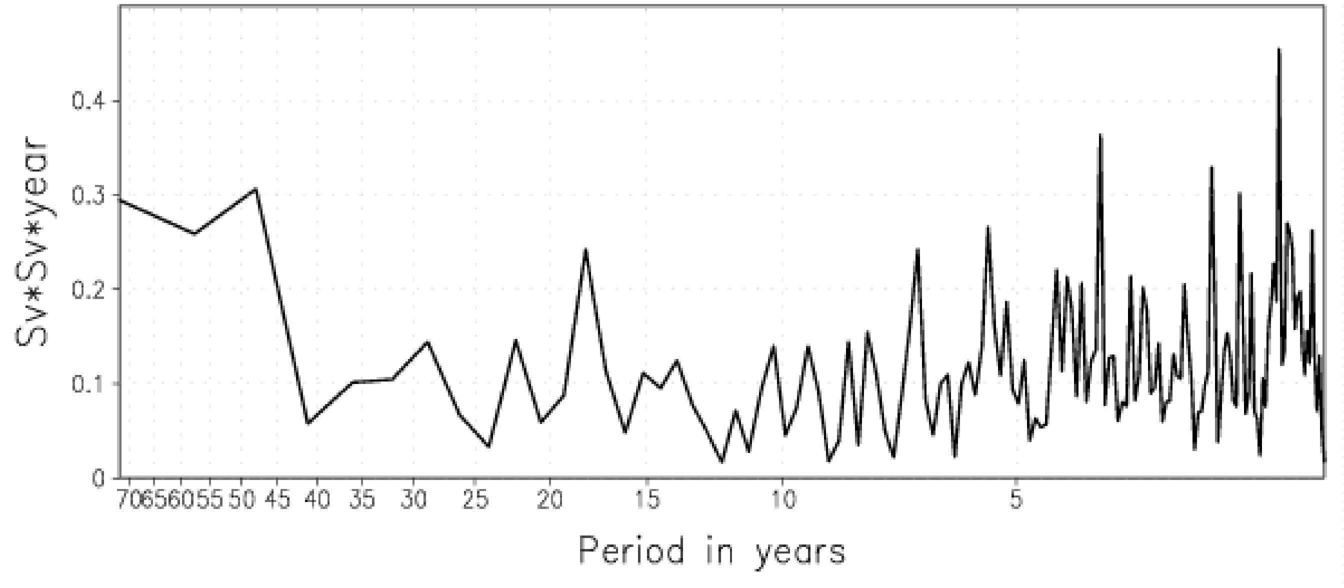

Significant long-period oscillations with periods around 50 and 18 years are marked out from the spectrum of anomalies of the annual average AMOC index allocated. Apparently at these time scales the circulation regimes in the North Atlantic may influence on the own climate change.

Conclusions

1. The results of simulating global ocean circulation and its interannual variability in 1948-2007 using INM RAS ocean general circulation model INMOM (Institute of Numerical Mathematics Ocean Model) are presented. The CORE datasets were used to set realistic atmospheric forcing.
2. Sea ice area decrease by 2007 was reproduced in the Arctic Ocean that is in good agreement with observations.
3. The interdecadal climatic variability was revealed with significant decrease of Atlantic thermohaline circulation (ATHC) and meridional heat transport (MHT) in North Atlantic (NA) since the late 1990's. MHT presents decrease of heat transport from NA to the atmosphere since the mid-1990’s.
4. Therefore the negative feedback is revealed in the Earth climate system that leads to reducing of climate warming caused primarily by anthropogenic factor for the last decades.
5. Long-term variability (60 years) of ATHC is revealed as well which influences NA thermal state with 10 year delay. The assumption is argued that this mechanism can make a contribution in the ATHC own long-term variability.


Thanks!

Sea ice concentration in March and September

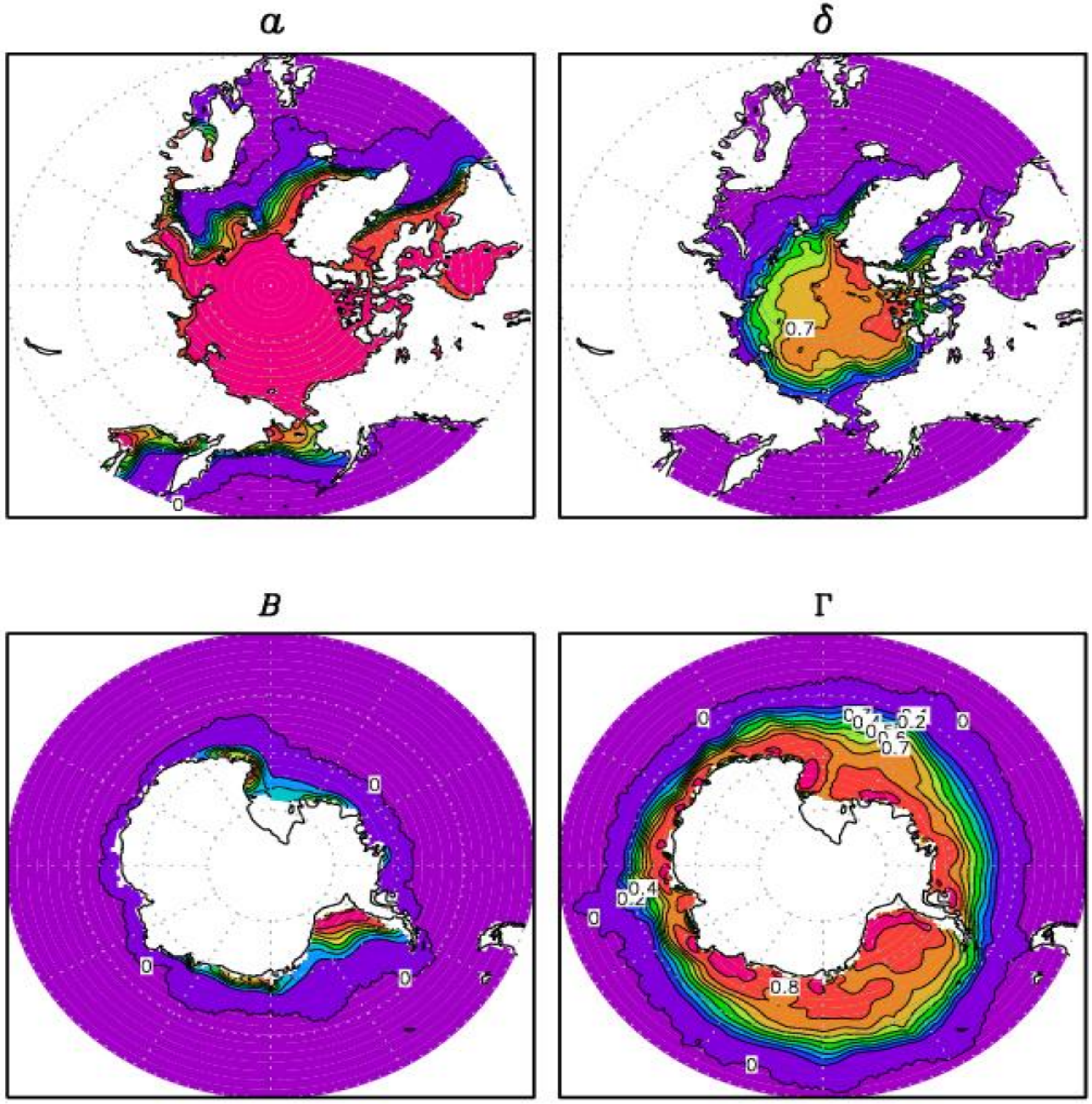

March ice square in Northern hemisphere, 10^6 km^

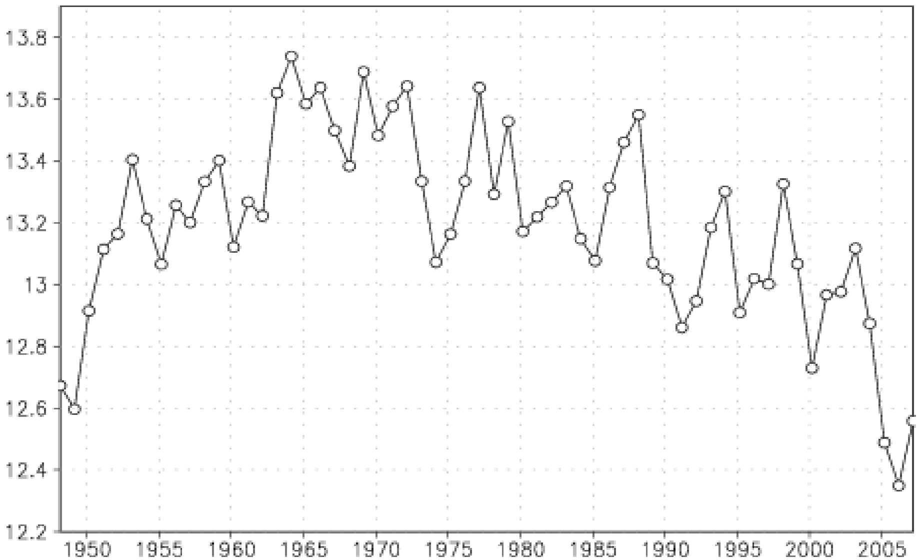

March ice volume in Northern hemisphere, 10^12 m^3

March ice square in Southern hemisphere, 10^6 km^

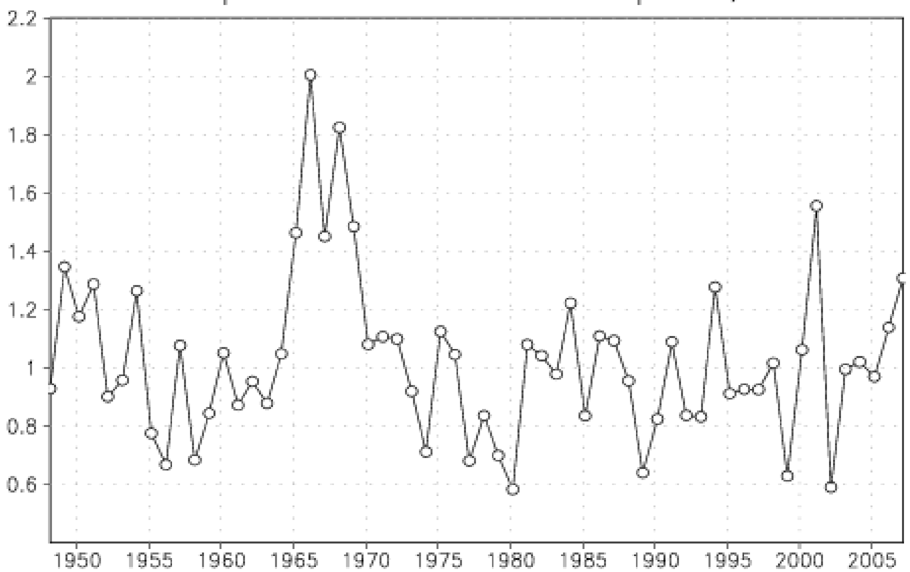

March ice volume in Southern hemisphere, 10^12 m^3

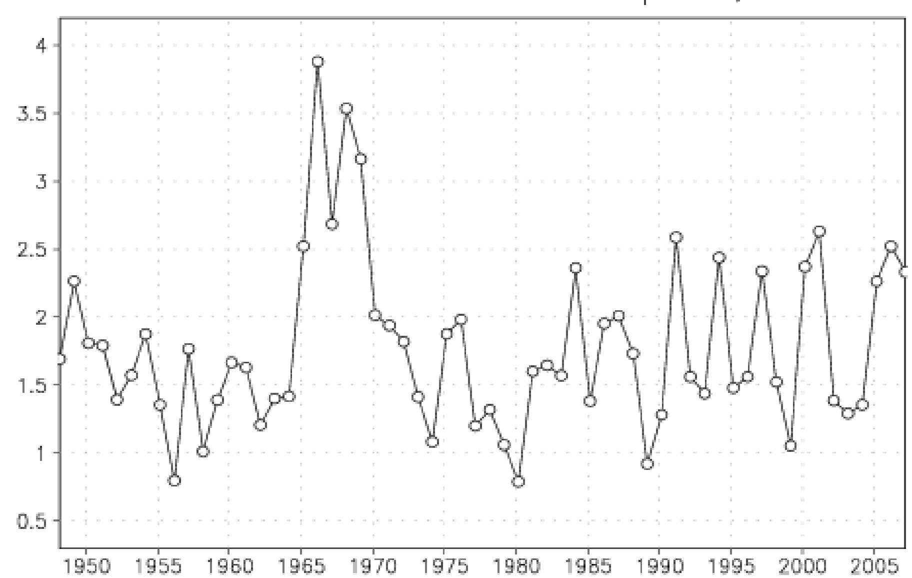

September ice square in Northern hemisphere, 10^6 kr

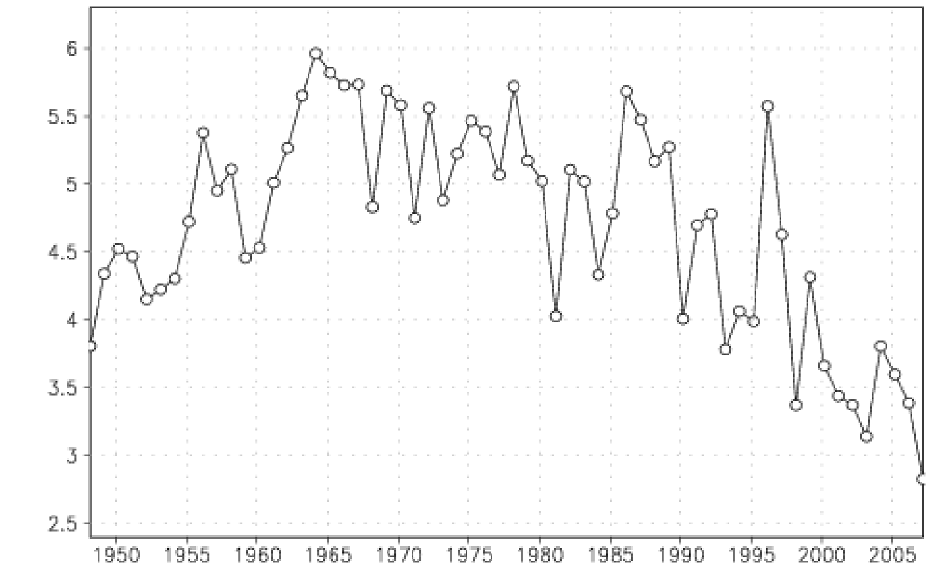

September ice volume in Northern hemisphere, 10^12 m

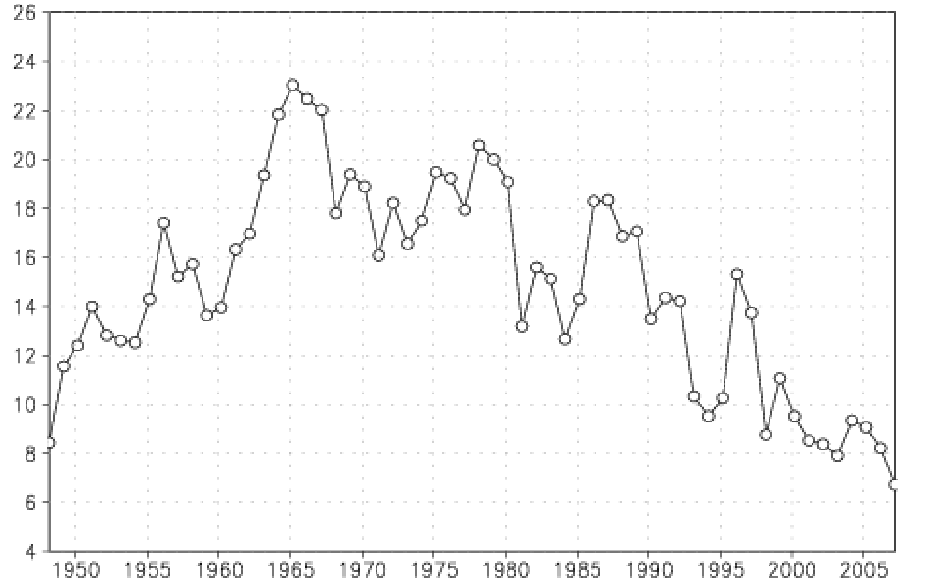

September ice square in Southern hemisphere, 10^6 kr

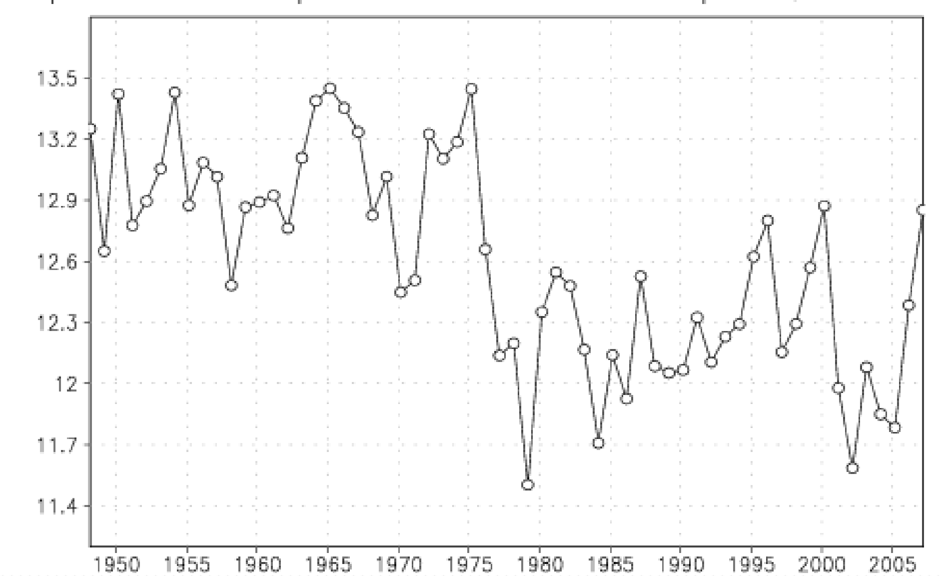

September ice volume in Southern hemisphere, 10^12 m

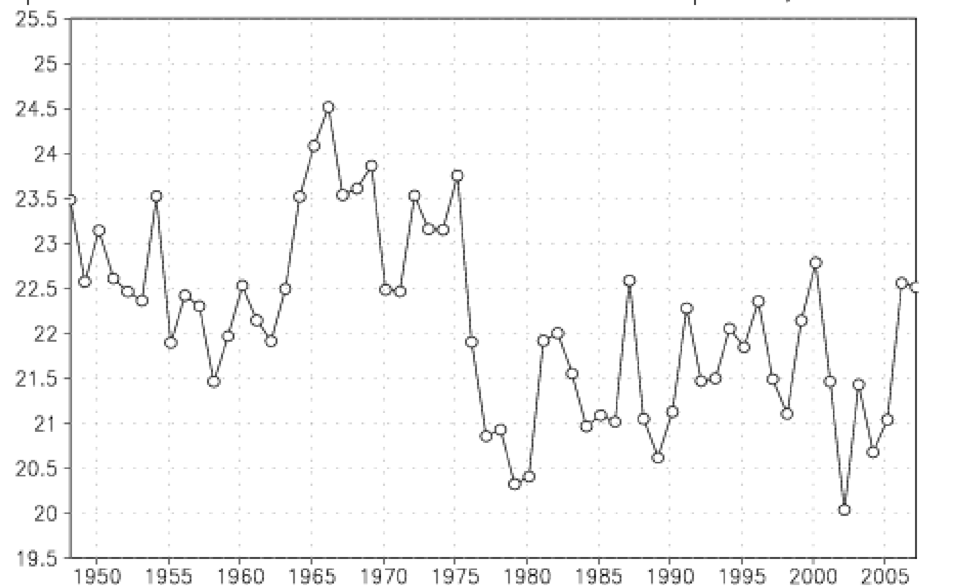

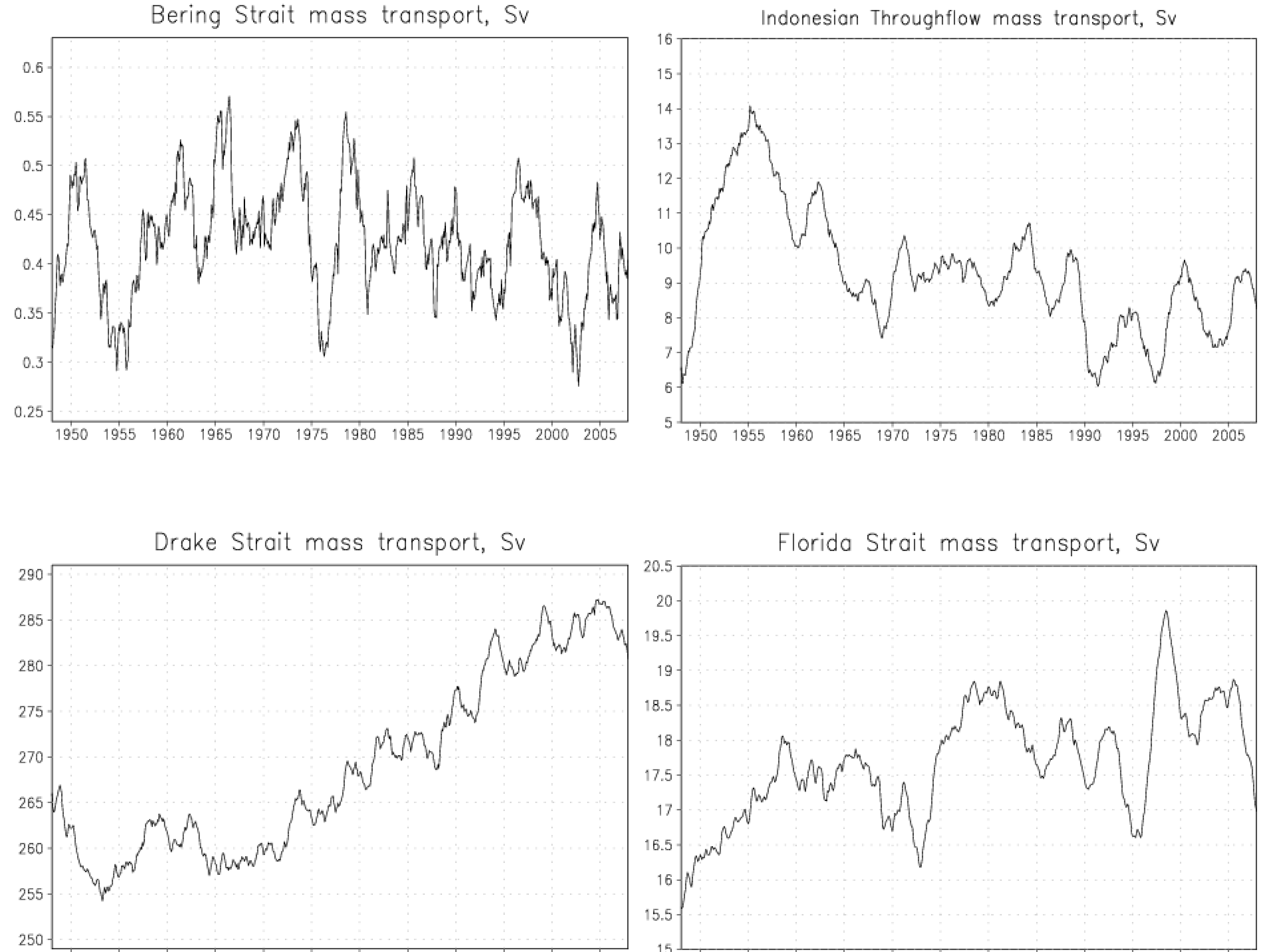
Bering Strait mass transport, Sv
0.6
0.55
0.5
0.45
0.4
0.35
0.3
0.25
1950 1955 1960 1965 1970 1975 1980 1985 1990 1995 2000 2005
Indonesian Throughflow mass transport, Sv
16
15
14
13
12
11
10
9
8
7
6
5
1950 1955 1960 1965 1970 1975 1980 1985 1990 1995 2000 2005
Drake Strait mass transport, Sv
290
285
280
275
270
265
260
255
250
Florida Strait mass transport, Sv
20.5
20
19.5
19
18.5
18
17.5
17
16.5
16
15.5
15